
C. de Tomás^{1,2}, A. Cantarero¹, A.F. Lopeandia², F.X. Alvarez²

¹University of Valencia, PO Box 22085, Valencia, 46071, Spain;

²Autonomous University of Barcelona, Bellaterra, Barcelona, 08193, Spain

LATTICE THERMAL CONDUCTIVITY OF SILICON NANOWIRES

We have calculated the lattice thermal conductivity of silicon nanowires using the Boltzmann transport equation for bulk phonons within the relaxation time approximation. The model includes anharmonic phonon scattering, both Umklapp and normal processes, the scattering of phonons due to isotopic disorder and the scattering by the boundaries, needed to avoid the divergence of the thermal conductivity at low temperatures. This minimum set of relaxation times allows us to verify the validity of the classical approaches in the study of the thermal conductivity of small diameter nanowires. From the comparison with experimental data for silicon nanowires, we conclude that the classical limit is valid for nanowires larger than 30 nm in diameter. There is no need to include the folding of acoustic phonons or confinement of optical phonons.

Key words: lattice heat conduction, semiconductor nanowires, Boltzmann transport equation.

Introduction

Semiconductors have a larger Seebeck (S) coefficient than metals and their thermal conductivity (κ) is not directly related to the electrical conductivity (σ) as is the case of the formers, through the Lorentz number $L = \kappa/\sigma T \approx 2.44 \times 10^{-8} \text{ W}\cdot\Omega/\text{K}^2$. The reason is that the heat flow in semiconductors is mainly due to phonons, i.e. the heat flow is dragged by the phonons, not by the electrons. The low carrier concentration as compared to metals makes the electrical contribution to the thermal conductivity negligible, at least in bulk materials. As it is well known, the fingerprint of this behavior is the typical T^3 law shown at low temperatures, instead of the linear behavior present in metals.

Actually, although for some applications it is important to have a large thermal conductivity in order to dissipate heat (microelectronic substrates, for instance), the large thermal conductivity of semiconductors is one of the drawbacks in the development of efficient thermoelectric devices. The reason is that the efficiency of a thermoelectric device is inversely proportional to the thermal conductivity. If we are able to decrease substantially the thermal conductivity, which in practice means to reduce it to that corresponding to the electronic contribution, we will drastically improve the efficiency of the thermoelectric device. Twenty years ago, Hicks and Dresselhaus [1] showed that the lattice thermal conductivity κ_L can be reduced by engineering different semiconductors or combining semiconductor alloys with different concentration in the form of superlattices. Quantum dots and, more recently, nanowires (NWs) are the subject of intensive research in the field of thermoelectricity [2].

The fast decrease of the thermal conductivity with decreasing nanowire diameter has been experimentally demonstrated [3]. On the other hand, several theoretical approaches have been published to account for the variation of κ_L with NW diameter [4-6]. In these works, phonon confinement, anharmonic processes by optical phonons at low temperature, or interface scattering with a variable specularity parameter, have been proposed to contribute to the lowering of the thermal conductivity in NWs. Unfortunately, several concepts have been used, many times with

unclear physical arguments: the need of a classical or quantum behavior, the presence of new scattering mechanisms like the decay of optical phonons into acoustical phonons, even at very low temperatures, interference scattering, while essential scattering mechanisms, like the existence of normal scattering processes, have been neglected. This panorama has contributed to mix up physical concepts and to the misunderstanding of the real physics behind the reduction of the lattice thermal conductivity in nanowires.

In the present work, we show that the behavior of the κ_L in semiconductor nanowires can be explained classically, in the whole temperature range, with an appropriate treatment of the different scattering processes, in particular the normal scattering processes, or N -processes. Phonon confinement, boundary scattering and other exotic processes are not necessary if the problem is correctly focused. The developed model predicts, using the parameters obtained from a fit of bulk silicon, the thermal conductivity of silicon nanowires down to 30 nm in diameter.

Lattice thermal conductivity derived from the Boltzmann transport equation

To deduce an eigenvalue solution of the Boltzmann transport equation (BTE), it is convenient to write it in terms of a symmetrized perturbed phonon distribution function,

$$N_q^*(r,t) = \frac{1}{2\sqrt{N_q^0(N_q^0 + 1)}} N_q(r,t), \quad (1)$$

where the equilibrium distribution function

$$N_q^0 = \frac{1}{e^{(\hbar\omega_q/k_B T)} - 1}. \quad (2)$$

In Eq. (2), the phonon branch has been omitted for simplicity. The BTE for phonons, in a symmetric form [7] is:

$$\frac{\partial N_q^*(r,t)}{\partial t} + v_q \nabla N_q^*(r,t) = - \sum_{qq'} S_{qq'}^* N_q^*(r,t). \quad (3)$$

The scattering matrix which appears in the right hand side of Eq. (3) is symmetric in q and q' . The left-hand side operator, containing the time derivative and the convective term with the group velocity, is named drift operator. In general, the scattering matrix is unknown, but we can write it as

$$S_{qq'}^* = N_{qq'}^* + R_{qq'}^* \quad (4)$$

separating the normal and resistive processes. As it is well known [8], N -processes do not contribute in a direct way to the thermal conductivity, they only redistribute the energy and momentum between the different phonon modes and give rise to a drifted distribution function when we are not far from equilibrium:

$$N_q^0 = \frac{1}{e^{(\hbar\omega_q - \mu q_0)/k_B T} - 1}. \quad (5)$$

At low temperatures, and neglecting boundary effects, we have partial information on the N -matrix, which appears in Eq. (4). Let us write the eigenvalue equation

$$\sum_{q'} N_{qq'}^* \phi_{q'}^\alpha = \lambda_\alpha \phi_q^\alpha. \quad (6)$$

It is straightforward to check that the matrix of the N -operator is diagonal and that there are, at least, four eigenvalues equal to zero. These eigenvalues correspond to the equilibrium distribution function given by Eq. (2) ($\lambda_0 = 0$) and to the drifted distribution function corresponding to Eq. (5) ($\lambda_1 = \lambda_2 = \lambda_3 = 0$). Thus, in the limit of low perturbation (low temperature gradient and low drift), the matrix corresponding to N -processes has the simple form [7]

$$N^* = \left(\begin{array}{c|ccc|c} 0 & 0 & 0 & 0 & 0 \\ 0 & 0 & 0 & 0 & 0 \\ 0 & 0 & 0 & 0 & 0 \\ 0 & 0 & 0 & 0 & 0 \\ \hline & & \lambda_4 & \lambda_5 & \lambda_6 \\ 0 & 0 & 0 & 0 & \ddots \end{array} \right) \equiv \begin{pmatrix} 0 & 0 & 0 \\ 0 & 0 & 0 \\ 0 & 0 & N_{22}^* \end{pmatrix},$$

where the eigenvalues can be written in terms of

$$\lambda_4 = \lambda_5 = \lambda_6 = \dots = \frac{1}{\tau_N} \quad (7)$$

the relaxation time in the limit where N -processes are dominant. On the other hand, the equilibrium distribution function is also an eigenvector of the R -operator with zero eigenvalue. The form of the BTE is, finally,

$$\left[\begin{pmatrix} 0 & 0 & 0 \\ 0 & 0 & 0 \\ 0 & 0 & N_{22}^* \end{pmatrix} + \begin{pmatrix} 0 & 0 & 0 \\ 0 & R_{11}^* & R_{12}^* \\ 0 & R_{21}^* & R_{22}^* \end{pmatrix} - \begin{pmatrix} D_{00}^* & D_{01}^* & 0 \\ D_{10}^* & D_{11}^* & D_{12}^* \\ 0 & D_{21}^* & D_{22}^* \end{pmatrix} \right] \begin{pmatrix} a_0 \\ a_1 \\ a_2 \end{pmatrix} = 0, \quad (8)$$

which gives rise to three equations:

$$\begin{aligned} D_{00}a_0 + D_{01}a_1 &= 0 \\ -D_{10}a_0 + (R_{11} - D_{11})a_1 + (R_{12} - D_{12})a_2 &= 0 \\ D_{21}a_1 + (N_{22} + R_{22} - D_{22})a_2 &= 0, \end{aligned} \quad (9)$$

where a_0 is a scalar, a_1 is a vector of order 3, and a_2 is a vector of infinite length. The dimensions of the matrices can be derived correspondingly. The eigenvectors a_j can be written, in general, as a linear combination of the eigenvectors of the N -operator. But, since we do not know a_2 , we can combine the last two terms of Eq. (9) and we will have, finally, a set of two equations [7], containing a_0 and a_1 , which gives rise to the energy conservation,

$$\frac{\partial \varepsilon}{\partial t} + \nabla j_\varrho = 0 \quad (10)$$

and to the vector equation

$$\frac{\partial j_\varrho}{\partial t} + \frac{1}{3} v^2 C_v \nabla T = -(\tau^{-1})_{11} j_\varrho \quad (11)$$

representing the momentum conservation. We have made use of the fact that $\nabla \varepsilon = C_v \nabla T$, C_v being the specific heat and v the average group velocity. The term multiplying the heat current can be called phonon momentum relaxation operator, and it can be written in terms of the 3×3 matrices:

$$\left(\tau^{-1}\right)_{11} = R_{11}^* - R_{12}^* R_{21}^* \left(N_{22}^* + R_{22}^*\right)^{-1}. \quad (12)$$

In the steady state, Eq. (11) can be inverted and define a thermal conductivity operator, which will be also a 3×3 matrix. Considering the heat flow in the same direction of the temperature gradient, it is easy to arrive to the expression

$$j_Q = -\frac{1}{3} C_v v^2 \tau \nabla T, \quad (13)$$

where the average

$$\tau = \frac{\int \tau \omega^2 \frac{\partial f}{\partial \omega} D(\omega) d\omega}{\int \omega^2 \frac{\partial f}{\partial \omega} D(\omega) d\omega}. \quad (14)$$

Going to the limit where N -processes dominate, the following equation can be deduced:

$$R_{11}^* = 1 / \langle \tau_R \rangle. \quad (15)$$

On the other hand, in the limit where N -processes are negligible,

$$R_{11}^{*-1} = \langle \tau_R \rangle. \quad (16)$$

We can combine the equations of the resistive matrix and its inverse and deduce the non-diagonal terms,

$$R_{11}^* = \sqrt{R_{11}^* \left[R_{11}^* - 1 / R_{11}^{*-1} \right]}. \quad (17)$$

The final expression of the momentum relaxation time is

$$\tau_{11} = \langle \tau_R \rangle \frac{\tau_N + \langle \tau_R^{-1} \rangle^{-1}}{\tau_N + \langle \tau_R \rangle} \quad (18)$$

and the thermal conductivity has the expression

$$\kappa = \frac{1}{3} C_v v^2 \left[\langle \tau_R \rangle (1 - \Sigma) + \langle \tau_R^{-1} \rangle^{-1} \Sigma \right], \quad (19)$$

where we have defined the switching factor

$$\Sigma = \frac{\langle \tau_R \rangle}{\tau_N + \langle \tau_R \rangle}. \quad (20)$$

At low temperature, when the N -processes dominate, the switching factor is 1 and the second term of the thermal conductivity expression is dominant. This temperature regime is called the Ziman regime [9]. On the other hand, when the normal processes are negligible (at very high temperatures) the switching factor is zero and the first term dominates. This is called the kinetic regime. The switching factor thus indicates the dominant regime and, depending on its value, the conductivity “switches” from one regime to the other.

In spite of the isotropic boundary relaxation time, it is convenient to introduce a geometrical factor taking into account the sample geometry. Guyer and Krumhansl [10] did it for cylindrical geometry, but in terms of a complicated expression containing cylindrical Bessel functions. Here, we have used a geometrical factor derived from non equilibrium irreversible thermodynamics for any geometry, in particular valid for nanowires [11]. The expression of the geometrical factor is very simple,

$$F\left(\frac{\ell}{L_{\text{eff}}}\right) = \frac{1}{2\pi^2} \frac{L_{\text{eff}}^2}{\ell^2} \left(\sqrt{1 + 4\pi^2 \frac{\ell^2}{L_{\text{eff}}^2}} - 1 \right), \quad (21)$$

where the phonon mean free path

$$\ell = v\tau \quad (22)$$

depends on the temperature through the scattering mechanisms (relaxation time) and L_{eff} is the effective size of the sample. In the case of nanowires, $L_{\text{eff}} = d$, the diameter of the nanowire. Since the mean free path of the phonons is much larger than the diameter of the nanowires, the geometrical factor will be basically

$$F\left(\frac{\ell}{L_{\text{eff}}}\right) = \frac{L_{\text{eff}}}{\pi\ell}. \quad (23)$$

Introducing the geometrical factor into the expression for the lattice thermal conductivity, we obtain

$$\kappa = \kappa_K (1 - \Sigma) + \kappa_Z F\left(\frac{\ell}{L_{\text{eff}}}\right) \Sigma, \quad (24)$$

which is the final expression used to calculate the thermal conductivity.

Lattice dynamics and phonon relaxation times

The lattice thermal conductivity is proportional to the average phonon group velocity. This is the reason why the acoustic longitudinal branches are contributing in great extent to the heat transport. Optical phonons do not contribute, basically, since the dispersion is very small. For a confident calculation of the thermal conductivity, a reliable model of the lattice dynamics is needed. In this work, we have used the bond charge model of Weber [12] and its original data. The advantage of the bond charge model is that utilizes a minimum set of parameters and reproduces quite well even the flat region of the acoustical branches close to the border of the Brillouin zone (BZ), and it can be extended to other technologically interesting compounds [13].

In undoped semiconductors, the most important scattering mechanisms are phonon-phonon processes or phonon anharmonicity. At high temperatures, the Umklapp processes are dominant. Recently, Ward and Broido [14] have performed ab initio calculations of the thermal conductivity of bulk silicon in the temperature range from 100 to 800 K. In this temperature range, boundary scattering is of no importance and was not taken into account. They deduced a functional form for the relaxation time of U -processes which has been corrected by us to account for the low temperature behavior (below 100 K):

$$\tau_U^{-1} = B_U \omega^4 T e^{-\Theta_U/T} \left[1 - e^{-3T/\Theta_p} \right]. \quad (25)$$

The extra term $e^{-\Theta_U/T}$ limits the efficiency of U -processes at low temperature. Since U -processes do not conserve momentum, the sum of three (or four) phonon wave vectors must be as large as a reciprocal lattice vector, and this is not possible at low temperatures. If we consider a phonon energy of the order of kT and draw a horizontal line in the dispersion relations, clearly the phonon wave vectors are far from the limit of the BZ. In order to select Θ_U and not to use it as a fitting parameter, we have divided the BZ into three and looked at the crossing point of the acoustical longitudinal branch, giving us a phonon energy, which can be transformed into temperature dividing the Boltzmann

constant. Concerning the relaxation time for N -processes, the expression of Ward and Broido [14] does not behave properly at low temperatures as well, where the temperature behavior must follow the T^3 law. We have added an extra term to account for this behavior:

$$\tau_N^{-1} = \left(\frac{1}{B_N T} + \frac{1}{B'_N T^3} \right)^{-1} \omega^2 \left[1 - e^{-3T/\Theta_D} \right]. \quad (26)$$

Silicon, or any other material, has an isotopic disorder in its natural form [15]. In particular, *Si* has only three stable isotopes, ^{28}Si , with 92.2297(7) % abundance, ^{29}Si , with 4.6832(5) % abundance, and ^{30}Si , with 3.0872(5) % abundance. The isotopic disorder is a very important mechanism in the undoped materials. Isotopically pure *Si*, for instance, has thermal conductivity one order of magnitude larger than natural *Si* [16]. A well established expression for isotopic disorder or mass defect scattering relaxation time is [17]:

$$\tau_I^{-1}(q) = A\omega^4(q) = \frac{V_0 g}{4\pi} \frac{\omega^4(q)}{v^3(q)}, \quad (27)$$

where the factor g gives the mass fluctuation,

$$g = \sum_i f_i \left(\frac{\bar{M} - M_i}{M_i} \right)^2, \quad (28)$$

f_i is the mass fraction, \bar{M} is the average mass and M_i is the mass of individual isotopes. Finally, in order to fit the low temperature region and limit the thermal conductivity to finite values, it is necessary to introduce a relaxation time to account for the boundary (otherwise the thermal conductivity diverges at low temperature) [9]:

$$\tau_B^{-1}(q) = \frac{v(q)}{L_{eff}}. \quad (29)$$

In the last two expressions, the parameters have been obtained from the literature. Our model has three parameters that correspond to the phonon-phonon relaxation times: B_U , B_N and B'_N .

Results and discussion

Figure 1 shows the fitting of our model, using Eq. (24) with the relaxation times given by Eqs. (25 – 27) and (29), for natural silicon. The Mathiessen rule has been used to calculate the average relaxation time. The experimental data are from Inyushkin et al. [16], which gives an effective length of the sample of 2.8 mm. The fitting of natural silicon provides us the following parameters: $B_U = 1.8 \times 10^{-46} \text{ s}^3 \cdot \text{K}^{-1}$, $B_N = 2.0 \times 10^8 \text{ s} \cdot \text{K}^{-1}$, and $B'_N = 1.9 \times 10^{-23} \text{ s} \cdot \text{K}^{-3}$. The dots in Fig. 1 correspond to the experimental data [16], while the solid line is the theoretical fit with the parameters given above. The two contributions, Ziman (dashed line – green on line) and kinetic (dotted line – navy on line), to the thermal conductivity have also been plotted in the graph. The Ziman contribution, dominant when the switching factor approaches 1, is the most important at low temperature, while the kinetic contribution ($\Sigma = 0$) is more important at high temperatures. However, in the temperature range starting in 50 K to higher temperatures, we can observe that both contributions are necessary to obtain a reasonable fit of the thermal conductivity. That means that N -processes are also important at high temperature. Actually, in the work of Ward and Broido [16], where both relaxation times have been depicted as a function of frequency, they are of the same order of magnitude in the region of 10 – 15 THz (at 300 K). Clearly, N -processes cannot be neglected even at room temperature.

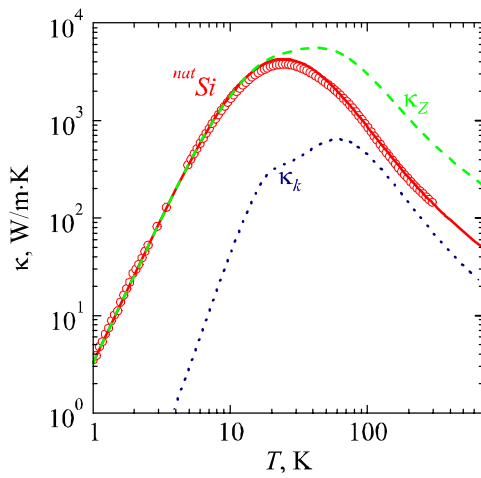


Fig. 1. Fitting of natural Si with the parameters given in the text. The open circles are the experimental data of Inyushkin et al. [16], while the solid line is the theoretical fitting. The dashed line (green online) is the Ziman contribution to the thermal conductivity, while the dotted line (navy online) is the kinetic contribution.

The contribution of isotopic disorder is concentrated basically in the region of 10 – 30 K, around the peak of the thermal conductivity. In the case of isotopically pure Si [16], only this region is affected by the disorder.

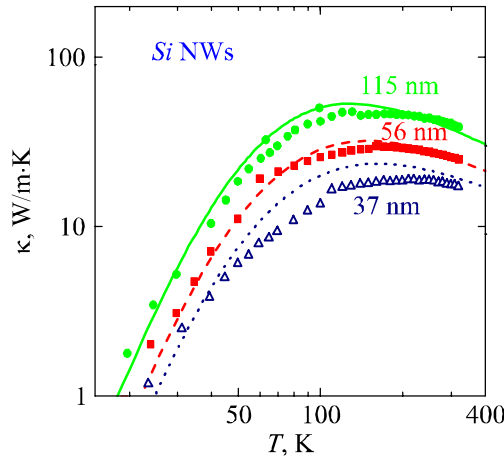


Fig. 2. Calculation of the thermal conductivity of nanowires with three different diameters using the model parameters obtained from the fitting of natural Si.

Figure 2 shows the calculated values of the thermal conductivity, using Eq. (24) with the parameters which fits the bulk silicon, for three different Si nanowires, with 115 (dots and solid line – green on line), 56 (full squares and dashed line – red on line) and 37 nm (up triangles and dotted line – navy on line). The only additional parameter which differs from the fitting to bulk silicon is the effective length of the sample, i.e. the diameter of the nanowire. At a given temperature (a given phonon mean free path), the thermal conductivity is reduced basically to the geometrical factor (in the approximated expression F is proportional to the nanowire diameter). By comparing the 115 nm NW with that of 37 nm, the reduction in the thermal conductivity at 50 K is two times larger than at room temperature. The reason is that at room temperature, the kinetic factor has a larger influence and the geometrical factor plays a smaller role. It was shown several years ago [18] that optical confinement in nanowires is important when the NW diameter is or the order of 2 – 3 nm. In the case of folded acoustic phonons, the experience can tell us that above 10 – 15 nm diameter, the number of phonon branches is so high that the use of a model considering the folding or a model considering bulk phonons will give a similar result on

the thermal conductivity. The essential points are the scattering mechanisms and, in particular, the correct treatment of N -processes, without neglecting the influence of the geometry.

Conclusions

A theoretical model able to predict the thermal conductivity of semiconductor nanowires has been proposed. The model considers properly phonon-phonon scattering. A geometrical factor has been included to account for the nanowire dimensions. A reliable model for the lattice dynamics with bulk phonons has been used. A minimum set of relaxation times has been taken into account in order to prove the validity of the model in the case of silicon nanowires down to 30 nm in diameter. Possibly, phonon folding effects are important below 10 – 15 nanometers.

Acknowledgements. The authors are grateful to the Ministry of Finances and Competitiveness of Spain for financial support through Grants CSD2010-00044 of the Programme “Consolider Ingenio 2010” and MAT2012-33483. Thanks are due to the University of Valencia for the use of the supercomputer TIRANT.

References

1. L.D. Hicks and M.S. Dresselhaus, *Phys. Rev. B* **47**, 16631 (1993).
2. J.P. Heremans, *Acta Phys. Pol. A* **108**, 609 (2005).
3. D. Li, Y. Wu, P. Kim, L. Shi, P. Yang, A. Majumdar, *Appl. Phys. Lett.* **83**, 2934 (2003).
4. M. Kazan, G. Guisbiers, S. Pereira, M.R. Correia, P. Masri, A. Bruyant, S. Volz, P. Royer, *J. Appl. Phys.* **107**, 083503 (2010).
5. P. Chantrenne, J.L. Barrat, X. Blase, J.D. Gale, *J. Appl. Phys.* **97**, 104318 (2005).
6. N. Neophytou, H. Kosina, *Phys. Rev. B* **83**, 245305 (2011).
7. R.A. Guyer, J.A. Krumhansl, *Phys. Rev.* **148**, 766 (1966).
8. I.G. Kuliev, I.I. Kuliev, *J. Exp. Theor. Phys.* **95**, 480 (2002).
9. J.M. Ziman, Electrons and phonons (Clarendon Press, Oxford), 1979.
10. R.A. Guyer, J.A. Krumhansl, *Phys. Rev.* **148**, 778 (1966).
11. F.X. Alvarez, D. Jour, and A. Sellitto, *J. Appl. Phys.* **105**, 014317 (2009).
12. W. Weber, *Phys. Rev. Lett.* **33**, 371 (1974).
13. J. Camacho and A. Cantarero, *Phys. Stat. Sol. (b)* **215**, 181 (1999).
14. A. Ward, D.A. Broido, *Phys. Rev. B* **81**, 085205 (2010).
15. F. Widulle, T. Ruf, A. Gobel, I. Silier, E. Schonherr, M. Cardona, J. Camacho, A. Cantarero, W. Kriegseis, V.I. Ozhogin, *Physica B* **263**, 381 (1999).
16. A.V. Inyushkin, A.N. Taldenkov, A.M. Gibin, A.V. Gusev, and H.J. Pohl, *Phys. Stat. Sol. (c)* **1**, 2995 (2004).
17. P.G. Klemens, Proc. Phys. Soc. London Sect. A **68**, 1113 (1955).
18. F. Comas, A. Cantarero, C. Trallero-Giner, M. Moshinsky, *J. Phys. Cond. Matt.* **7**, 1789 (1995); F. Comas, C. Trallero-Giner and A. Cantarero, *Phys. Rev. B* **47**, 7602 (1993).

Submitted 30.05.2013.